

Multi-Beam Range Imager for Autonomous Operations

Neville I. Marzwell
Jet Propulsion Laboratory
California Institute of Technology
4800 Oak Grove Drive
Pasadena, CA 91109

H. Sang Lee, R. Ramaswami
Science & Engineering Services, Inc.
4040 Blackburn Ln. Ste. 105
Burtonsville, MD 20866

511-36
N 93-22160
150-85
P. 8

Abstract

For space operations from the Space Station Freedom the real time range imager will be very valuable in terms of refuelling, docking as well as space exploration operations. For these applications as well as many other robotics and remote ranging applications, a small portable, power efficient, robust range imager capable of a few tens of km ranging with 10 cm accuracy is needed. The system developed is based on a well known pseudo-random modulation technique applied to a laser transmitter combined with a novel range resolution enhancement technique. In this technique, the transmitter is modulated by a relatively low frequency of an order of a few MHz to enhance the signal to noise ratio and to ease the stringent systems engineering requirements while accomplishing a very high resolution. The desired resolution cannot easily be attained by other conventional approaches. The engineering model of the system is being designed to obtain better than 10 cm range accuracy simply by implementing a high precision clock circuit. In this paper we present the principle of the pseudo-random noise (PN) lidar system and the results of the proof of experiment.

1. Introduction

The pulsed laser ranging system has been limited in use because of its complexity, size, and cost. Generally the system consists of a high power pulsed laser(s), large optics, complex electronics and elaborate data systems. Consequently, the system is bound to be large in size and weight, consume high power, and prone to frequent breakdowns. The conventional cw FM laser radar technique is limited in terms of range and resolution due to limited frequency chirping (~ 100 GHz) and laser mode bandwidth (~ 200 MHz). The best resolution expected in this technique is only about a few thousandths of the range coverage. This technique relies on analog signal processing which requires a large return signal. The noise bandwidth is fully open in these techniques, unlike in the preferred pseudo-random noise (PN) modulation [Golomb, 1965] cw lidar system.

To overcome these difficulties and to develop a maintenance-free, operational system for mission oriented applications, a PN cw lidar system is being developed by Science & Engineering Services, Inc., MD using commercially available diode lasers. Unlike the pulsed laser radar, whereby the range is determined by the direct measurement of the transit time of a short ($\sim 10^{-9}$ sec) high power laser pulse, the disclosed PN cw laser radar measures the target distance by measuring the time shift of the return signal modulation sequence with respect to the reference modulation sequence which is the same as the transmitter modulation sequence. The time shift is measured by invoking the cross correlation of the return signal with the reference modulation sequence and determining the time shift needed to bring the return code train in phase with the reference modulation sequence. The cross correlation between the reference modulation sequence and returned signal train becomes maximum for the correct time shift, while is virtually zero for other time shifts. This correlation technique using PN code is a powerful method to measure the weak return signal buried in a random noise background because of the phase sensitive detection capability of the correlation process. In terms of the sensitivity of the measurement, this technique is the counterpart of the phase sensitive detection technique of differential signal measurement-the correlation technique is a most general case of the phase sensitive technique. The power of a 150 mW AlGaAs diode laser that is commercially available at present, is equivalent to the average power of 1.5 MW peak power pulsed laser operating at 10 Hz, commonly used in pulsed lidar systems. Thus, the maximum range measurable by the proposed PN cw lidar, in principle, is no less than the conventional high power pulsed lidar systems. A factor of 10 or more improvement in the diode laser power is anticipated in the near future. This offers a potential for a factor 10

improvement in range resolution for the same integration time, or reduction of the signal integration duration for the same resolution.

2. Description of the System

The sensor system block diagram shown in Fig. 1., consists of three sub-systems: a diode laser transmitter, scanner & receiver optics, and detector and signal processing electronics which are controlled by a system computer. In the baseline mode, the diode laser is digitally modulated by a pseudo random code of a given length (10 bit) and 1 μ sec modulation time bin-width employing a modulator providing a 150 m quantization precision and 150 km unambiguous range coverage. After a fixed number of modulation periods(defined as a cycle in this disclosure), the modulation start time delay is readjusted by a prescribed manner using a delay generator to provide a phase shift between the cycles (typically an order of 10 periods) of the PN code. This phase information is then retrieved by the correlation calculation process and used to enhance the range resolution in the disclosed system in a unique way. The transmitter beam is deflected by the scanner to the target, and the return signal is deflected by the scanner to the receiver optics. This signal is measured by a detector/preamp unit to provide a low noise electronic signal. This signal is then further amplified and filtered by a postamplifier-filter unit. The gain of the post-amplifier is automatically adjusted to provide a proper signal level for the ADC by an AGC unit. The dynamic range of the ADC is not limited to be very low due to the specific features of the signal processing routine of the disclosed system whereby the ADC output is first summed at the accumulator. After accumulating the data for a preselected number of cycles, the time integrated digital signal from the accumulator is read into the correlator for the calculation of the correlation distribution and determination of the precise range.

The range is determined based on the correlation calculation as follows: The PRM cw Lidar relies on the delta function property of the autocorrelation function of a PN code. The cross correlations of the return signal with the reference modulation code are calculated for each of the n time bin shifts which cover the entire code length. Due to the delta function property of the PN code, the cross correlation is always zero except for the case in which a null phase difference between the transmitted code and received signal is realized. A null phase difference is realized for the time shift that corresponds to the round trip transit time between the transmitter and the target. Thus, the time shift that corresponds to the maximum cross correlation value gives the range of the target. Further analytical description of the technique used in this system is discussed below. Consider a cyclic, digital (1 or 0) nth order PN code represented by a_j . The cross correlation ρ_j of this code with another expression of PN code a'_j with elements 1 and -1, in place of 1 and 0, will then satisfy the following relationship:

$$\rho_j = \sum_{i=0}^{N-1} a_i a'_{j+i} = \begin{cases} (N+1)/2 & \text{for } j = 0 \\ 0 & \text{for } j \neq 0 \end{cases}$$

The return signal, s_j , acquired at the receiver is the convolution of the transmitter signal, $x_j = Pa_j$, and the target response R, thus

$$s(i) = \sum_{i=0}^{N-1} x_{i-j} R + b$$

where b represents the background and noise signal. Let P stand for the diode laser power. If we accumulate the data acquired for M periods of PR code cycle, the integrated signal, S, is

$$S(i) = \sum_{k=1}^M s_{i+(k-1)N}$$

The target signal and range is then derived by taking the cross correlation of the return signal with the reference modulation sequence which is shifted by l time steps relative to the return signal as

$$\rho_l = \sum_{i=0}^{N-1} S_i a'_{i-l} = M \left[P \frac{(N+1)}{2} R + b \right]$$

where $l = 2(d/c\Delta t)$, the number of modulation shifts during the round trip transit time to the target at distance d , and Δt is the modulation clock period which is referred to the time bin width in this disclosure. For any other shift the correlation becomes zero. Note since b is an uncorrelated noise signal, the correlation with "a" becomes almost zero. Therefore, by finding the correct shift for the maximum correlation, the distance to the target can be derived.

However, the number of ones in a sequence of an M-code always exceeds the number of zeros by one as an intrinsic property. Therefore the background term b can not be neglected for excessively noisy data. A new modulation code, A-code [Nagasawa, 1990] which corrects this defect is implemented in this disclosure, by slight modifying the M-code. As far as the noise reduction is concerned, the correlation technique with this new code is identical to the case of the phase sensitive technique.

Although the diode output can be modulated much faster than a few GHz and signal processing system permits a speed as high as 100 MHz, the signal to noise ratio decreases as the modulation speed increases. Under this constraint, the baseline of the disclosed system is a 1 MHz modulation with a flexibility of successively switching it to 10 MHz and 100 MHz modulation for short range measurements. Based on 1 MHz modulation frequency, this technique will provide 150 m range quantization precision. Further improvement of range resolution beyond the quantization precision can be achieved without increasing the clock speed by employing a novel digital range resolution enhancement technique. This technique is implemented by introducing a known delay time at the start of each code sequence, then averaging the digitized signal to obtain a higher resolution than the quantization precision. The delay time can either be a systematic delay with higher timing precision (e.g. 100 nsec step for 1 MHz system) spanning 0 to a few time bins of the modulation, or a delay by a larger time step (e.g. 300 nsec) for spanning 0 to a few tens of modulation time bins. The correct range is calculated by multiplying the speed of light and the weighted average of the time shifts in the correlation calculation using the integrated signal. The correlation value is used as the weighting function in this averaging process. A small random time jitter which is characterized by a uniform distribution of delay can also be used for improving the range resolution. Due to the random distribution of the delay, the average range calculated from the L cycles of the PN code will then provide a higher range resolution, $15/L$ meter. With this technique, for a 10 msec averaging, the net resolution of the 10 MHz system, with 15 km unambiguous range, can be as high as 15 cm. For a smaller unambiguous range a shorter PN code may be used, thus facilitating a higher range resolution inversely proportional to the number of cycles L , achieving a 3 cm resolution for an 8 bit code.

A schematic of the timing diagram of transmitter modulation, analog to digital converter (ADC) synchronization as well as the accumulator and correlator operation is shown in Fig.2. The first trace 1 represents the uninterrupted master clock sequence of a given speed. The second trace 2, represents the sequence of the ADC start trigger pulse which repeats for every M cycles of the clock period. After K periods of the modulation ($M \times K$ clock pulse periods), the delay change is reset to a new value as shown in trace 4. This delay value will be remained fixed for the next K periods as shown in trace 3. For every ADC start pulse, the accumulator is re-phased as shown in trace 6 to integrate the return signal for the exact modulation period. The accumulator dump pulse is triggered after L cycles of delay change and synchronized with the immediately following ADC start pulse as shown on trace 7. Total L number of different delay values are reset for one correlation calculation and measurement of a high resolution range as shown in trace 8. The cross correlation can be calculated efficiently by a computer algorithm, if the maximum required range is less than a few tens of km's and the resolution requirement is relaxed. However, for a high resolution and large range coverage whereby the required information processing volume is prohibitive, a hardware correlator module such as TRW TMC2023 can be employed for high speed calculation. When the time delay is going through the change, the continuity of the transmitter modulation becomes interrupted for a few bin periods. However, the reference modulation which relies on the ADC start signal is still contiguous and the noise reduction property of the PN modulation technique remains valid with the disclosed technique. Only a small fraction of the return signal is lost in this process as indicated in the figure.

Based on the assumed configuration: transmitter power of 150 mW; 20 cm receiver aperture; and PN modulation of 1 μ sec time bin, the signal from a target of 0.5 reflectivity at a distance of 15 km is estimated to be 5 photon per bin. This amounts to 4,400 photons for a 10 msec signal integration time. Any small detectable signal can be enhanced by the accumulation of data, while the random noise component is suppressed by the PN modulation correlation technique. Since the system is expected to be photon limited, the targets at a distance of 150 km is well within the ranging capability of the system simply by switching to a longer time-bin mode and integrating the return signal for

a longer period. As the target approaches to a short distance (for example less than 15 km), the master clock is switched to 10 MHz to obtain 15 cm resolution for a 10 msec integration. The clock speed switches further to obtain better resolution as the target reaches a near field (<1.5 km). Since the signal amplitude varies as an inverse square function of the range, the integration time at near field can be shortened to less than a msec without increasing any other parameters of the sensor, thus, facilitating a faster scanning of the object at a close distance. The baseline receiver optics consist of a scanner, a 20 cm diameter telescope, a bandpass filter with less than 1.0 nm bandwidth for suppression of the background radiation, and an Si Avalanche Photodiode (SiAPD). The collimating lens is used as a narrow band filter and is followed by a focusing lens. The detector array which consists of a number of detectors arranged in a row vertical to the optical plane is located at the focal plane of the lens. In this way each detector collects the return signal from a predetermined field of view covered by one of the multi-beams of the transmitter. Thus scanning the multi transmitter beam and receiver FOV by the common scanner in a direction perpendicular to the detector array axis, this system scans a wide field of view (FOV) to provide range data within.

3. Proof of Principle Experiment

Proof of principle experiments have been carried out utilizing a target board at Goddard Space Flight Center and an existing lidar system at GSFC (P/T lidar). A PN modulated diode beam of 10 mW at 790 nm is sent out to the target and the return signal is received by a 10x20 cm² aluminum mirror. A multi-alkali PMT is used to detect the signal with substantially deteriorated sensitivity from the that of optimum wavelength. The signal is then digitized by the modified P/T lidar data acquisition system which was designed for the pulsed system. The data is then averaged for 10 periods of modulation with different delay values respectively. The correlation calculation is performed on this data for accurate range measurements. The reference point near the transmitter is independently measured by placing a corner cube reflector at 2 m distance from the transmitter, thus the range value is the differential range between the corner cube and the target. The experiment was carried out using various modulation frequencies between 1 MHz and 10 MHz with various delay times.

A typical return signal from the target at 850 m range is shown in Fig.3a. For a given modulation, a set of delay times is introduced at the beginning of the modulation train and the return is averaged before the correlation calculation to imitate the signal processing of the real time system to be developed. The typical correlation values of the return signal are plotted in Fig.3b. The accurate range obtained from the correlation values are summarized in Table I and also plotted in Fig.4. We note that thus measured range is self consistent throughout the various modulation frequencies. It is very important to note that the range measured with 5 MHz modulation and 10 nsec step delay agrees with that of 10 MHz and 10 nsec delay within 1.2 m which is well within the maximum error due to the time resolution. This result clearly demonstrate that the ultimate range resolution is determined by the time resolution of the delay regardless of the modulation speed. Furthermore it validates the range resolution enhancement technique implemented. A commercial time delay generator chip with 50 psec precision is readily available and is planned to be implemented in our engineering model.

4. Recommended Commercialization Approach

There is a unique advantage to our PN lidar system over other systems including pulse system and frequency chirped lidar system. These are namely the long distance ranging capability and the high range resolution capability with Science & Engineering proprietary range enhancement technique. With a moderate diode laser power and moderate size optics, the PN lidar system can achieve a few tens of km's distance ranging while the resolution is kept to better than 10 cm level. The proof of concept experiment shows a robust performance of the system concept without optimization of the system parameters, indicating the robustness of the technique used here. The approach to the commercialization will begin with a single beam portable system development following this program for ground based ranging and speed detection applications in terms of automobile speed enforcement, altimetry, civil engineering survey, as well as collision avoidance where the range resolution of 10 cm is satisfactory over a few km distance. The next step in the commercialization is the further enhancement of the resolution to a few mm at near distance of less than a meter for process control in manufacturing industries. The range imaging and robotics application will follow this phase naturally. One of the important steps in this development is micro-packaging the system. Since the system is based on the digital concept, the electronics can be packaged into one board size with a special DSP microprocessor chip. For a near distance (a few km's) operation, the optics can be substantially small (~50 mm) and readily packaged into a portable size. We plan to draw JPL's expertise in this area to speed up this process.

5. Applications

A wide range of application is covered by this system. Although some applications require a relatively complex multi-beam system, many commercial applications need only a single beam baseline system. We envision a commercial product that is cost effective, due to the continuous reduction in laser cost, micro-packaging and micro-electronic fabrication, as well as the anticipated growth of the market for the proposed product. Some potential commercial applications of this sensor are as follows:

- i) Robotics Application - As an active range imager for recognition, pose estimation and ranging. Combined with passive camera video imaging, the data can facilitate a high speed high resolution processing. At short distances, range resolution of less than 1 mm is possible with this system.
- ii) Ranging Application - This includes applications in commercial aviation as well as navigation of surface vessels. Future environmental disasters such as the Alaskan oil spill can be prevented by employing this type of sensor. A cost effective version of this system has enormous commercial potential as an automobile collision prevention device for autonomous navigation of ground vehicles using the GPS system. A further development of the system as a civil engineering survey instrument used for accurate remote measurement of distance is also promising, because of its low cost and portability unlike the other systems currently available. Use of this system in police speed guns for vehicle speed violation detection is also very promising due to its accuracy and long range capability without it being detected by a radar detector.
- iii) Aerosol and Wind Sensing - This type of laser radar can be used to measure the wind and aerosol field within the range of a few km's. With Doppler frequency shift measurements that can be easily accomplished utilizing a stable diode laser frequency, the baseline sensor can be directly applied to the development of a compact Doppler wind sensor.
- iv) Environmental Application - This sensor can also be the baseline of an environmental sensor for remote monitoring of industrial smoke and urban smog. This sensor can be further modified and developed to be used as an active gas sensor for measuring many environmental gases.
- v) Communications Application - Some of the parameters of this system are of interest for a highly directional communication system, including the frequency stabilization, receiver system design, and modulation technique. Short range exclusive communications may also be possible by tuning the laser output frequency to a specific atmospheric trace gas absorption line thus shielding the signal beyond a certain range.
- vi) Airborne altimeter applications - This sensor, when used in the altimeter mode, can measure the forest timber volume by integrating the tree height information. The airborne altimeter application is also very useful for an areal surface topography, mapping, and land and soil management when integrated with a GPS system.
- vii) Industrial manufacturing applications -for surface inspection to determine surface flaws and component defects, like solder joints, cracks, dents; in metrology to measure hole diameters, lengths, widths, thickness; in guidance and control for part sorting, palletizing, pick and place operations, insertion and removal; in integrity and placement verification to determine if a feature lies within specified bounds.
- viii) IFF application - as a small, low power, robust system for a highly effective Identification Friend or Foe system in the battle field.
- ix) Medical application - in measuring fluorescence decay and photon migration signature of tissue cells for cancer detection and other disease monitoring.
- x) Emerging space applications - reconnaissance and docking operations, health status monitoring of space vehicles.

Acknowledgement

The research described in this paper was partially carried out by the Jet Propulsion Laboratory, California Institute of Technology, under a contract with the National Aeronautics and Space Administration. This work was funded by a NASA Small Business Innovative Research Contract, NAS7-1186. The development and commercialization is being carried out at the SESI, Burtonsville, MD.

REFERENCES

Golomb, Solomon W., "Digital Communications with Space Applications", Peninsular Publishing Company, Los Altos, California, 1964.

Nagasawa, C. M., Abo, H. Yamamoto, and O. Uchino, "Random modulation cw lidar using new random sequence," Applied Optics, Vol.29, No.10, 1990.

Table 1. List of measured target ranges for various system parameters.

Measured Range (m) vs Number of delays

# DELAY	$F_T = 1 \text{ MHz}$	$F_T = 5 \text{ MHz}$	$F_T = 10 \text{ MHz}$
0	803.4 \pm 165 854.3 \pm 30	831.0 \pm 16.5 842.9 \pm 30	834.2 \pm 16.5 846.7 \pm 30
10	876.7 \pm 30	842.5 \pm 3 853.5 \pm 16.5	841.2 \pm 3 848.1 \pm 16.5
20	N/A	N/A	853.3 \pm 15.7

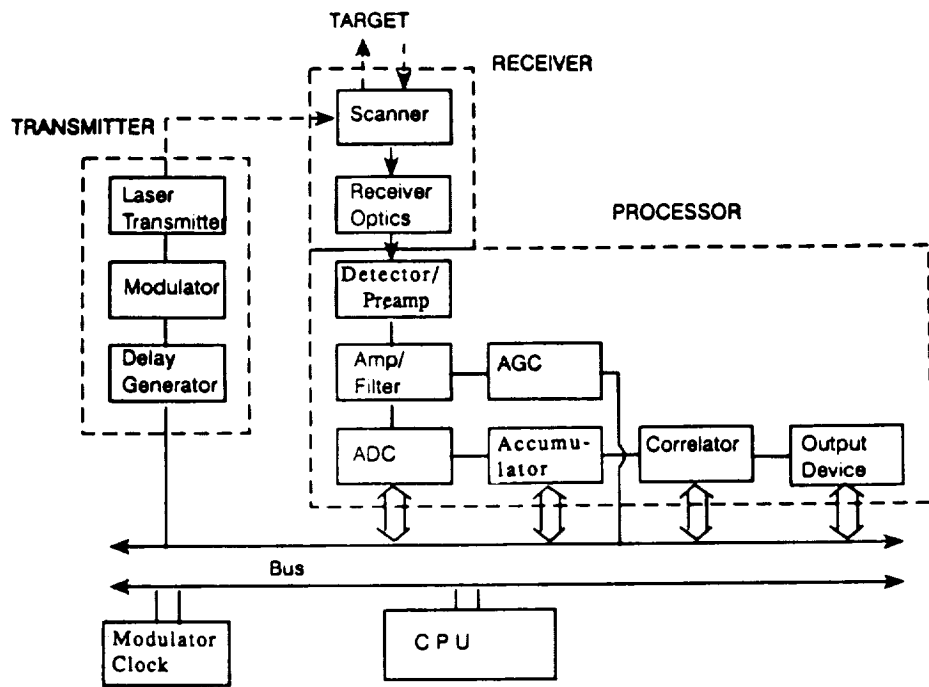


Fig. 1 Schematics of PN lidar system for accurate range imaging applications.

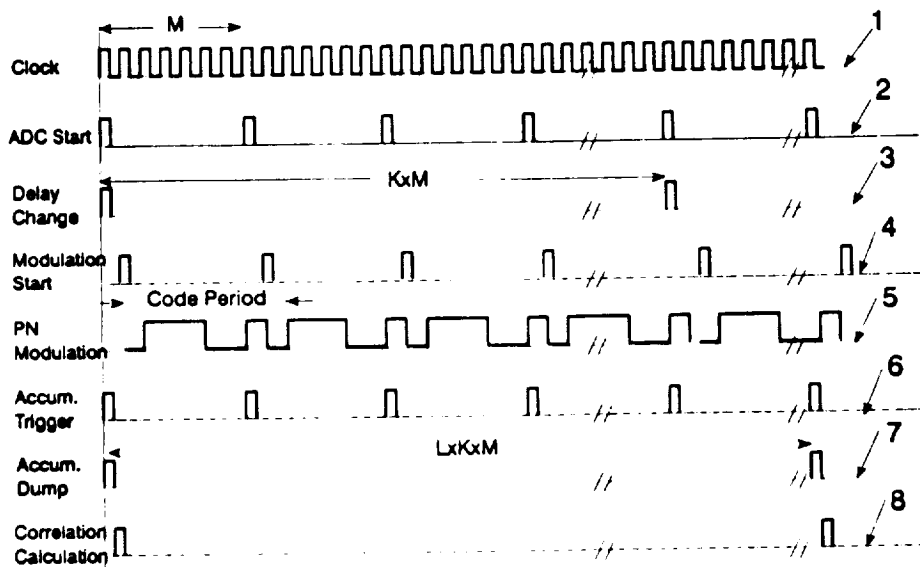


Fig. 2 Timing diagram for PN lidar system implementing the range-resolution-enhancement technique.

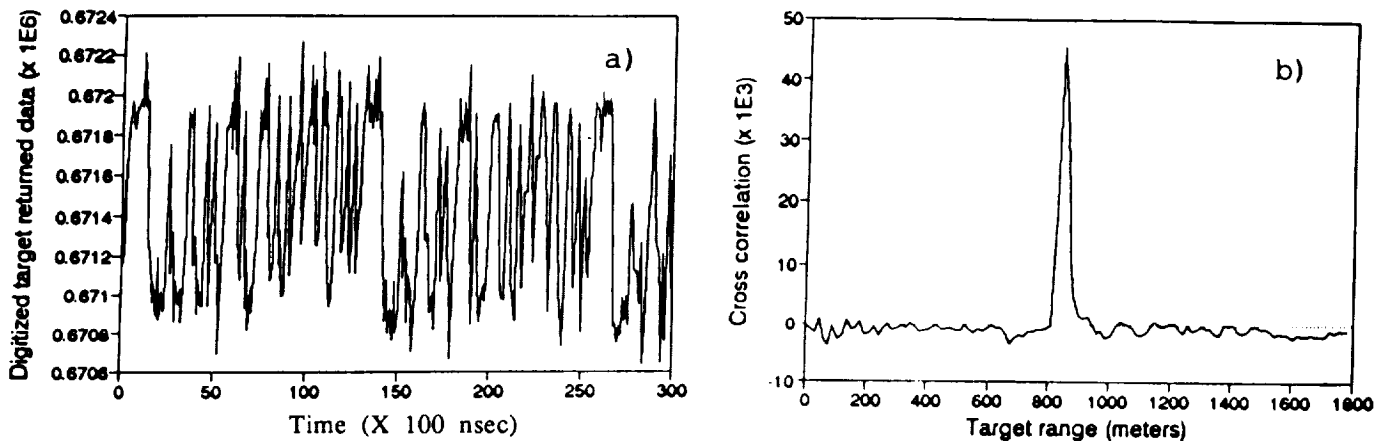


Fig. 3 a) Measured return signal from a target at a distance of 841.7 m, using a 10-mW diode laser 10 x 20 cm² optics.
 b) Correlation calculated from the measured data shown above.

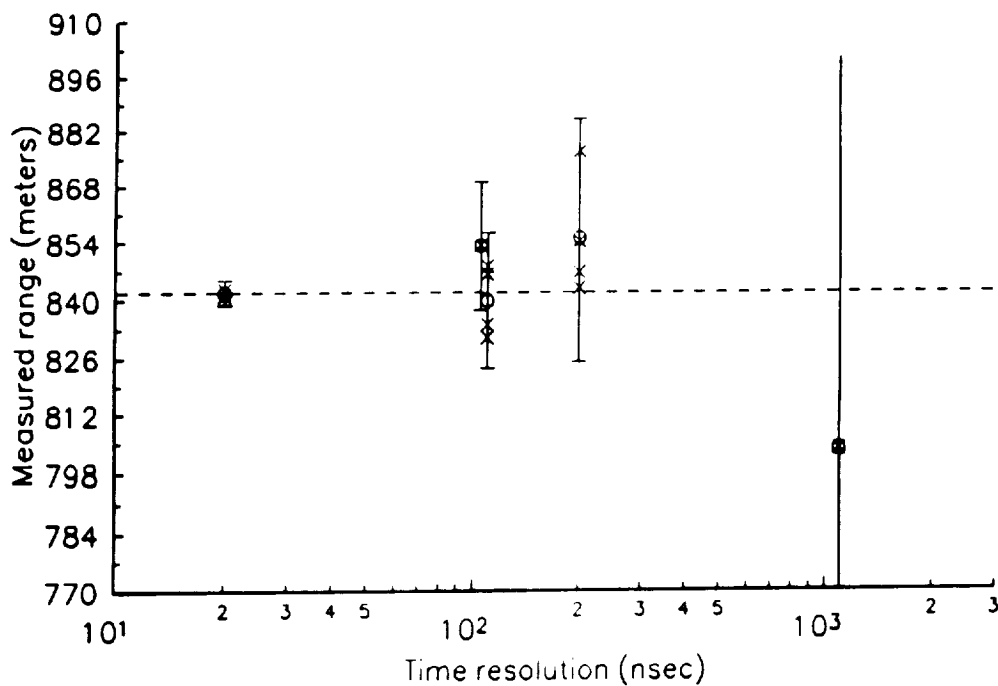


Fig. 4 A plot of measured target range for various system parameters. The "x" points correspond to each data set, and "o" symbols with the indicated error bar represent the average range value for a given time resolution. The time resolution is accomplished either by the system clock frequency or by the delay precision used in the range-enhancement technique. The two data points on the left that are in agreement within 1.3 m correspond to 10-MHz and 5-MHz clock frequency, respectively, and 10-nsec delay precision.